

# Selective contacts for undoped photovoltaic cells fabricated by high pressure sputtering

F. Pérez-Zenteno<sup>1</sup>, E. García-Hemme<sup>1</sup>, E. San Andrés<sup>1</sup>, R. Benítez-Fernandez<sup>1</sup>, G. Godoy-Pérez<sup>1</sup>, I. Torres<sup>2</sup>, R. Barrio<sup>2</sup>, D. Caudevilla<sup>1</sup>, S. Duarte-Cano<sup>1</sup>, R. García-Hernansanz<sup>1</sup>, J. Olea<sup>1</sup>, D. Pastor<sup>1</sup>, A. del Prado<sup>1</sup>

<sup>1</sup>Dpto. EMFTTEL. Fac. de Ciencias Físicas. Universidad Complutense de Madrid. Avda. Complutense s/n. Ciudad Universitaria. 28040 Madrid. Spain. e-mail: francp05@ucm.es  
<sup>2</sup>Unidad de Energía Solar Fotovoltaica, Dpto. de Energías Renovables, CIEMAT. Av/ Complutense 40, E-28040 Madrid, Spain

## Motivation

Explore materials ( $\text{TiO}_x$ ) to build an alternative structure of solar cells (Dopant Free Asymmetric Heterojunction - DASH) by the unconventional technique of High-Pressure Sputtering (HPS)

Overcoming intrinsic limitations of homojunctions and HIT solar cells. **Cheaper and sustainable solar energy.**

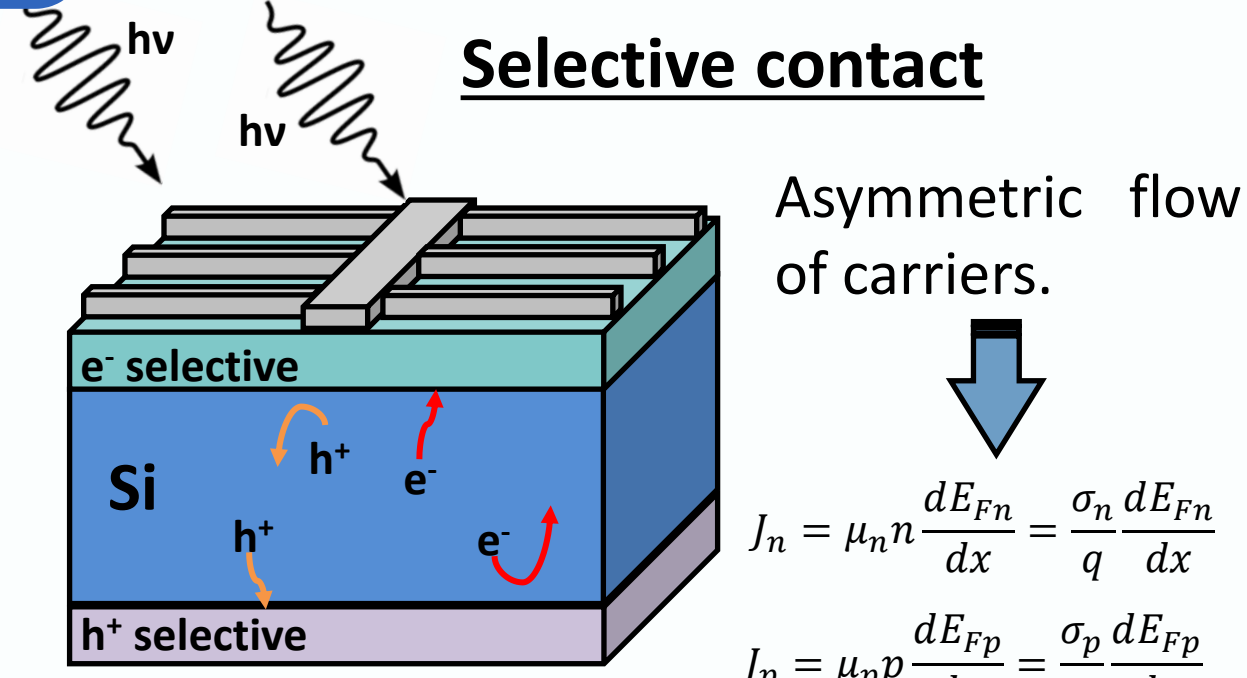
Why high pressure?

- Hazardous gaseous precursors
- High temperature processes
- Parasitic absorption

Minimize substrate damage by thermalization of sputtered species.

$$\lambda = \frac{kT}{\sqrt{2\pi}d^2p}$$

K - Boltzmann const. [J/K]  
 T - Temperature [K]  
 d - Kinetic diameter [pm]  
 p - pressure [Pa]



Energy bands bending with high band gap materials (TMO)

- Easy to produce
- Low cost (low temperature processes)
- Plenty of materials

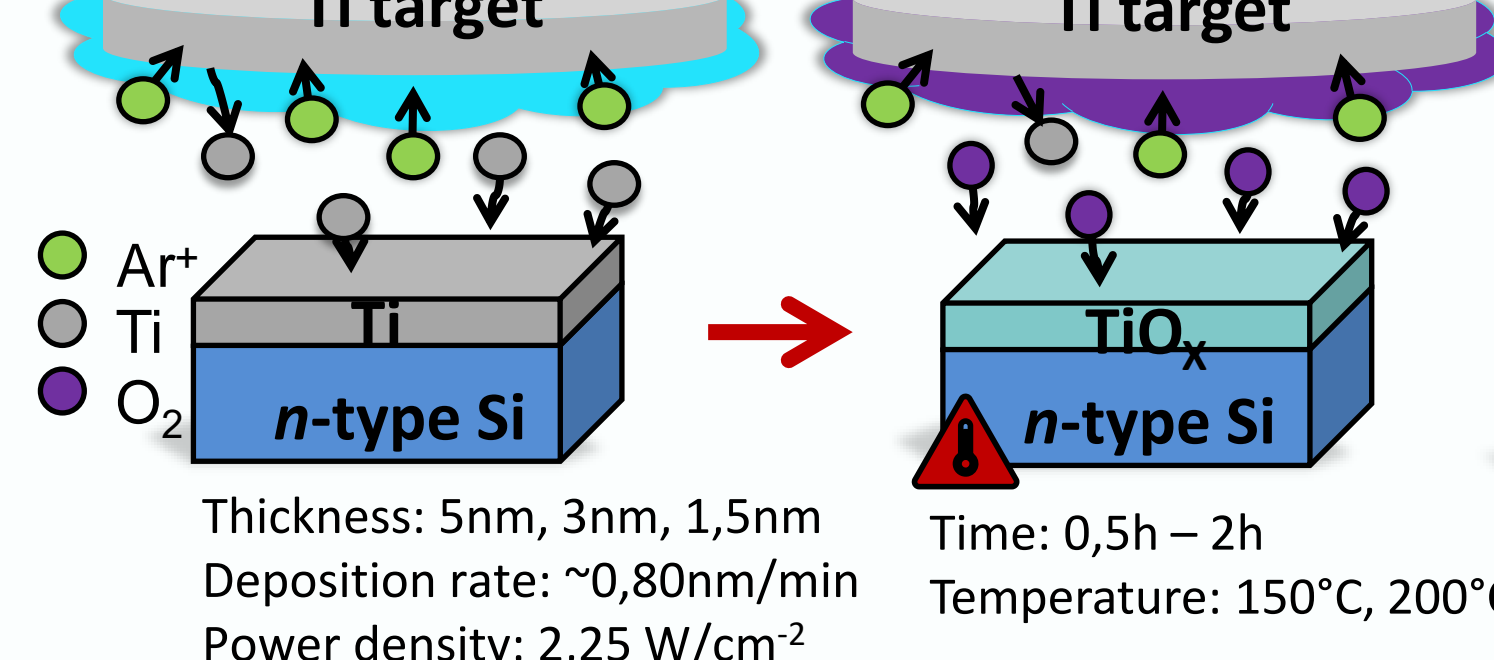
## Experimental

### Fabrication process

Deposition of  $\text{TiO}_x$  at 0,5mbar 45W by HPS. To achieve good selectivity and conductivity

Two-step deposition method:

Ti deposition + thermal/plasma oxidation



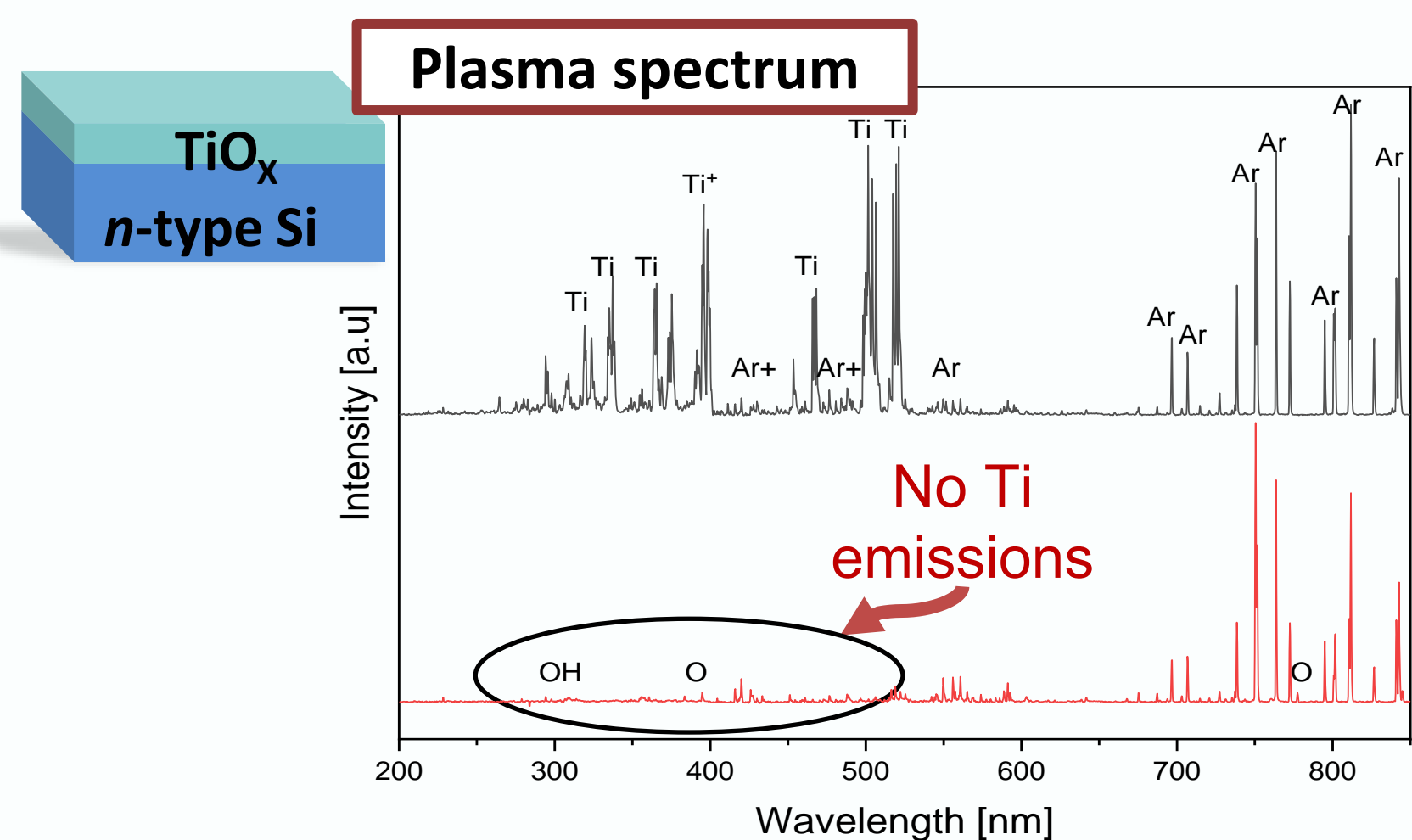
### Structural characterization

- XPS → Oxidation states, stoichiometric factor
- FTIR → Chemical bond vibrations
- Ellipsometer → Refractive index, thickness
- TEM → Crystal structure, thickness

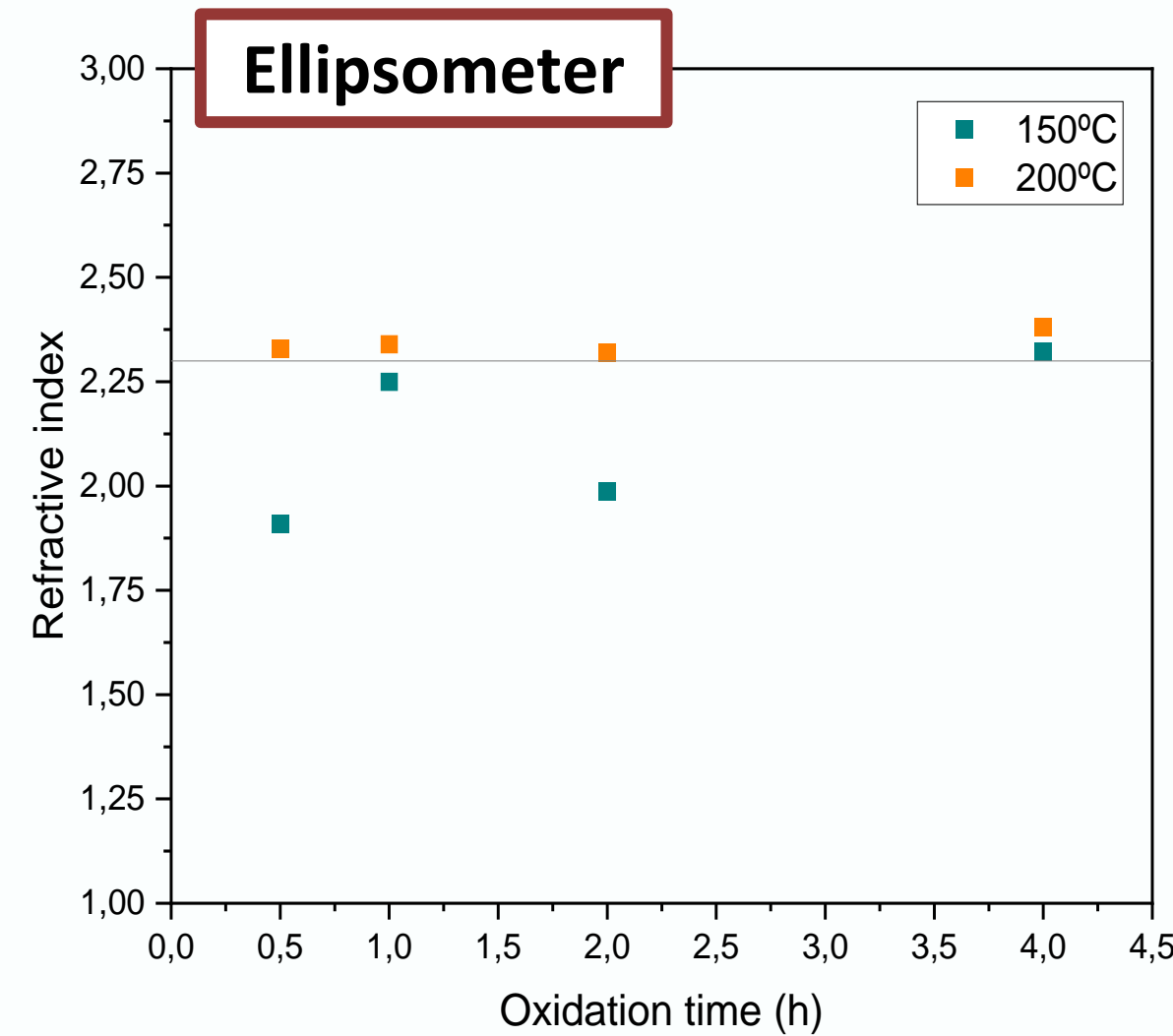
### Electrical characterization

Cox&Strack → Specific contact resistivity [ $\rho_c$ ] measurement  
 $R_T \approx \frac{\rho_w}{\pi d} \arctan\left(\frac{4t}{d}\right) + \frac{\rho_c}{4} \pi d^2 + R_o$   
 QSS-Photoconducance → Carrier lifetime

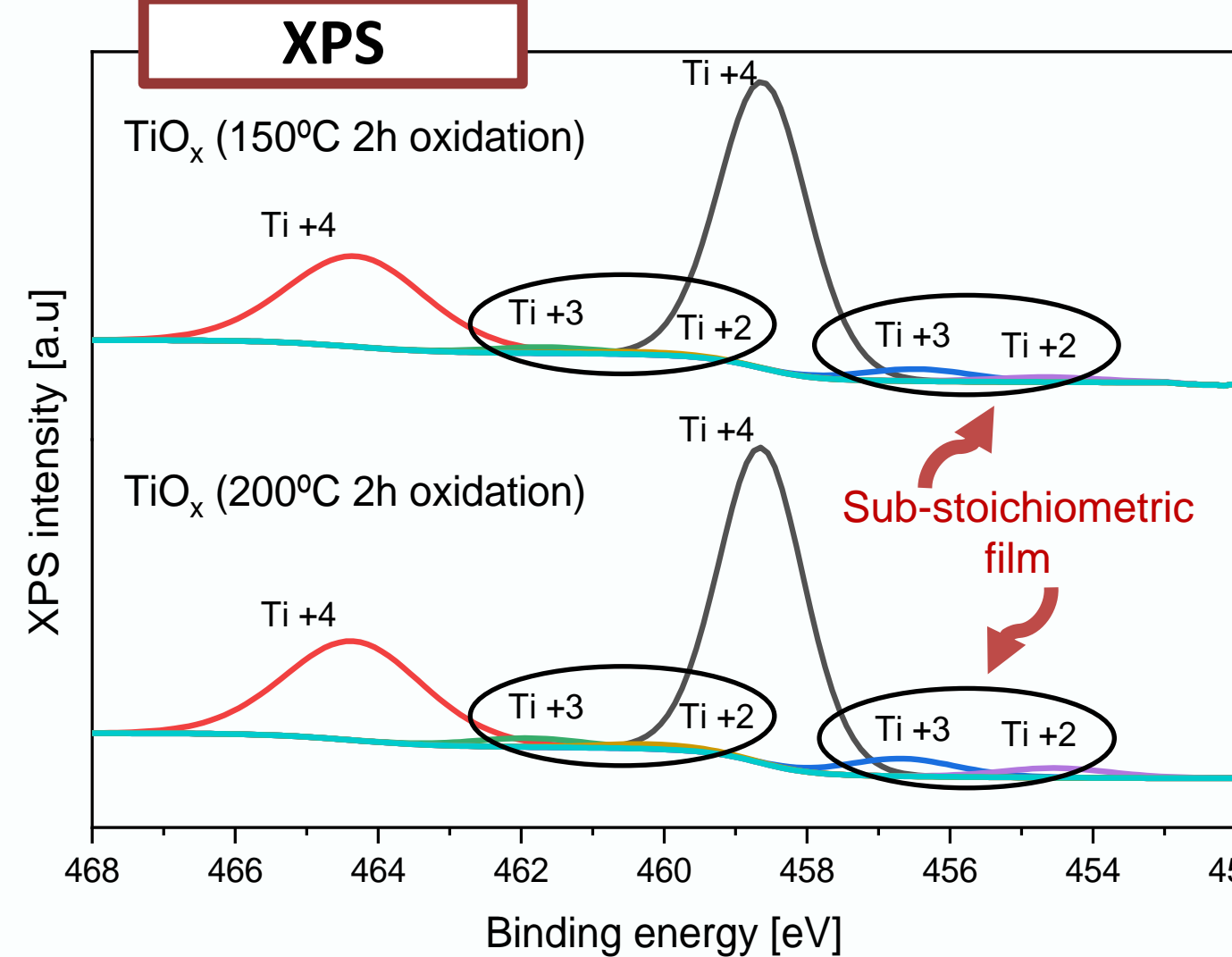
## Results



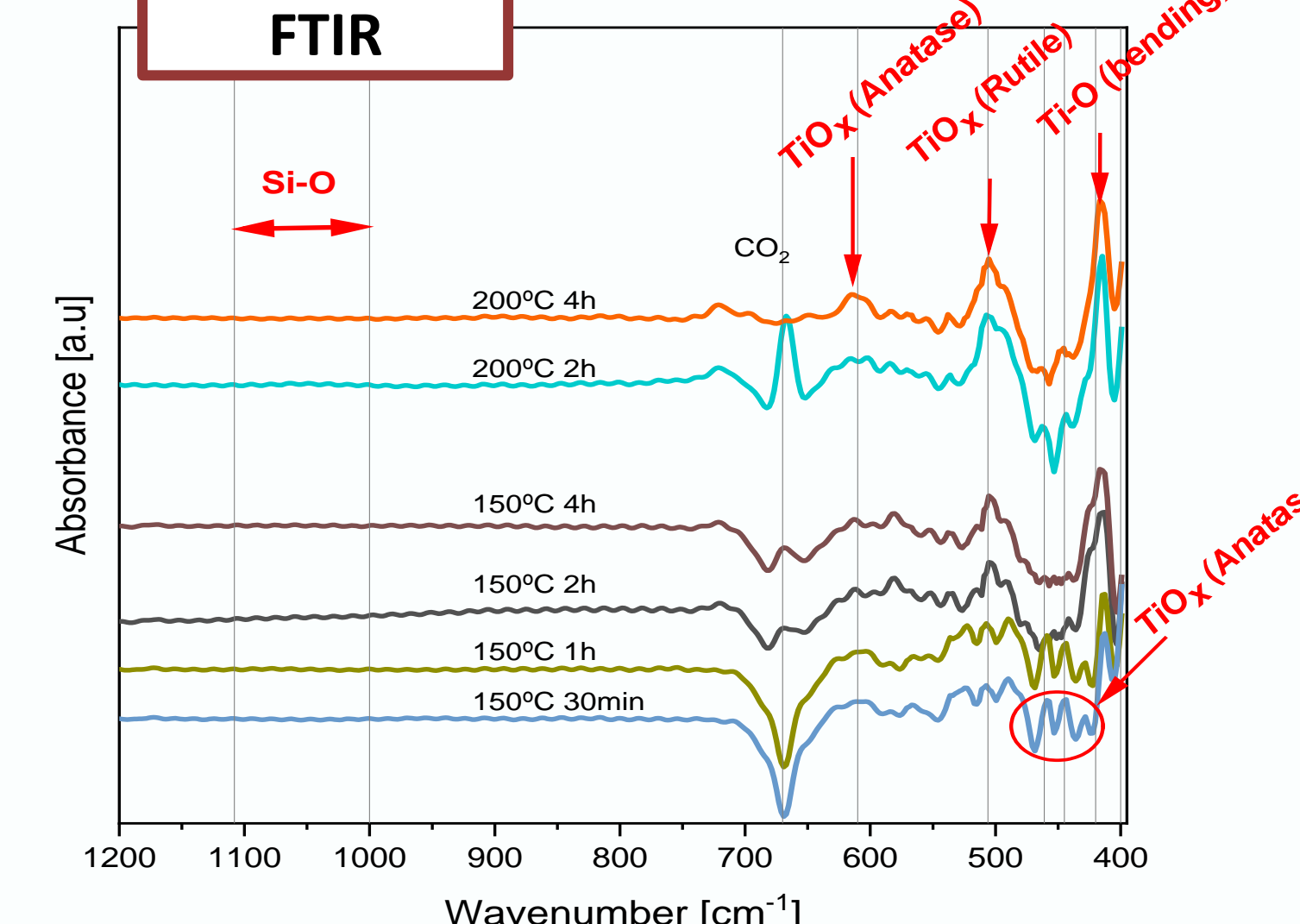
Characterization of plasma processes. In step 2, no Ti emissions are observed (no Ti deposition). Previous vacuum and target conditioning are extremely important.



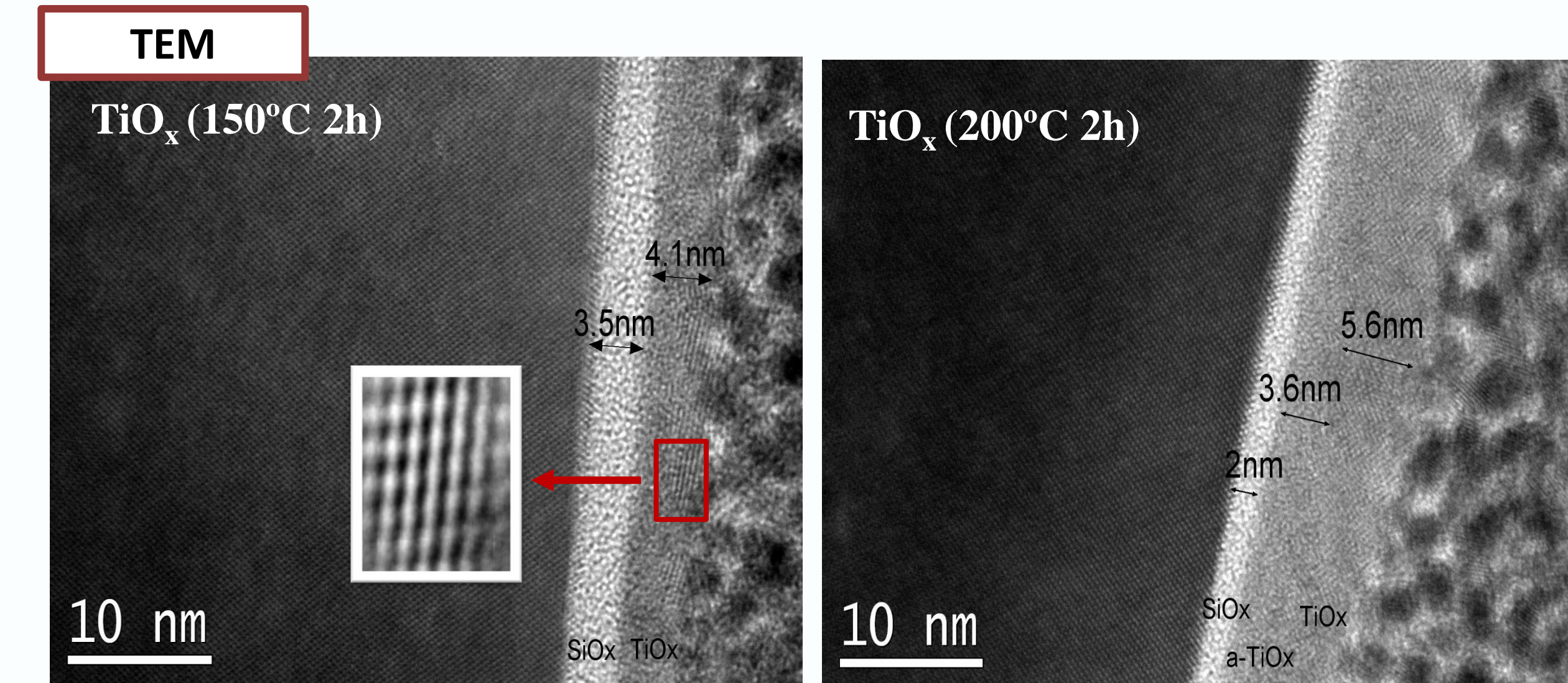
Modification of the refractive index (n) of  $\text{TiO}_x$ . According to [1] thermal ALD  $\text{TiO}_x$  n ~ 2,3 (at 632nm).



Characteristic doublet of Ti (+4) oxidation state at 464 eV and 458 eV. However, the Ti(+3) and Ti(+2) are also present. Oxygen to Ti ratio (x) of ~ 1,94.



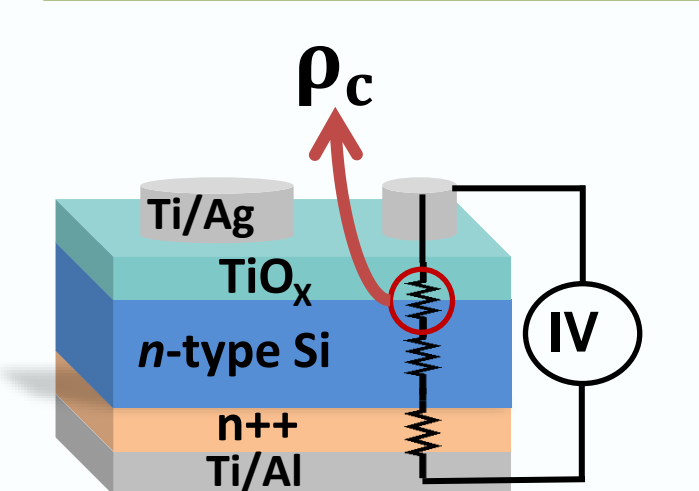
No significantly Si-O absorption is detected. This might indicate minimal oxidation in the substrate. [2]



TEM image shows an amorphous  $\text{TiO}_x$  with some regions that portray embedded nano crystal. Furthermore, a thin  $\text{SiO}_x$  film has regrown, probably due to the diffusion of  $\text{O}_x$  inside de Ti film.

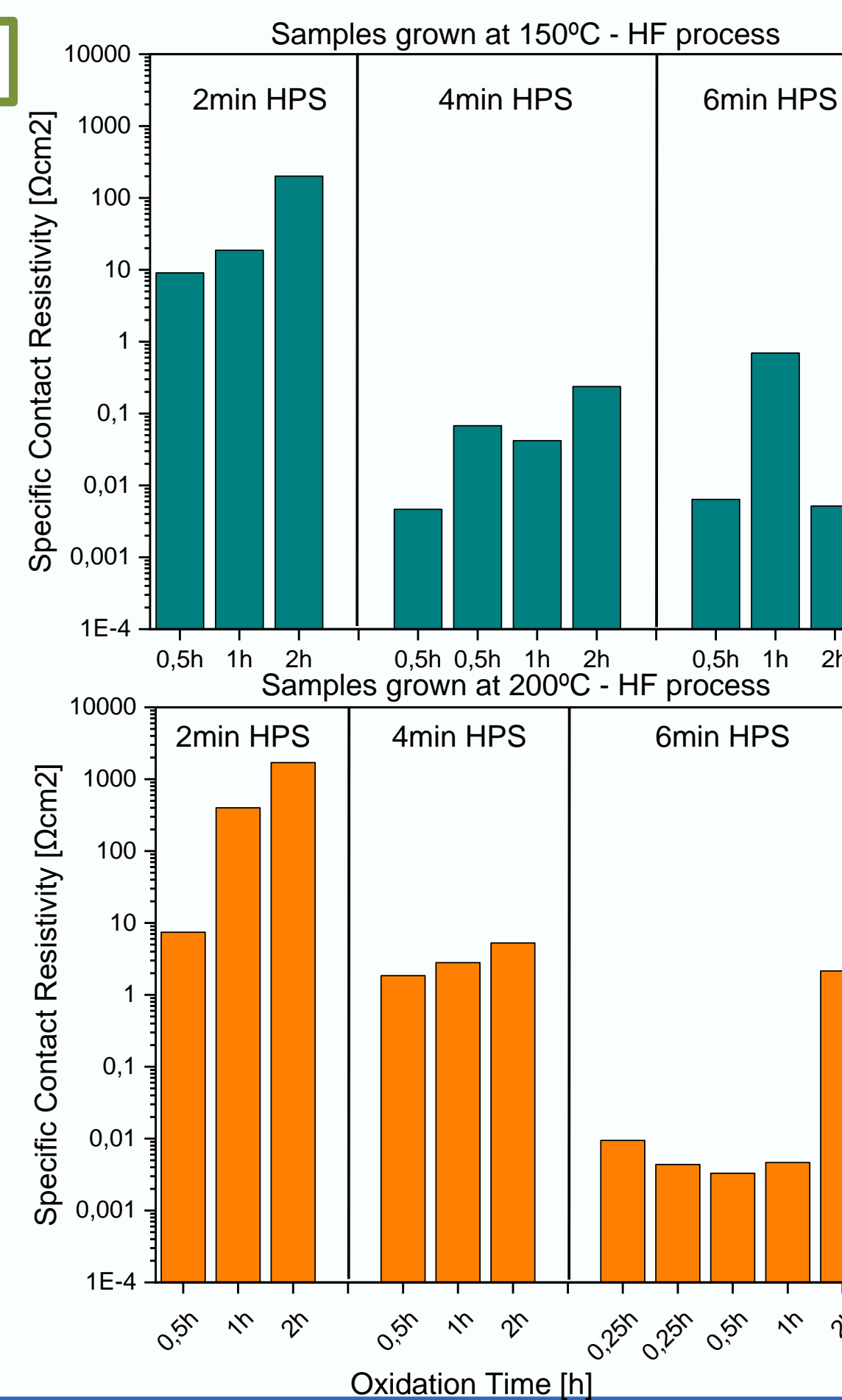
At 200°C, two different Ti layers appears to emerge. On the surface, there is a crystalline layer. In the middle an amorphous layer is observed.

### Cox&Strack



Cox&Strack samples to measure the  $\rho_c$  of  $\text{TiO}_x$ /n-Si junction. Three different sputtering time (6min, 4min and 2min), each one grown at 150°C or 200°C.

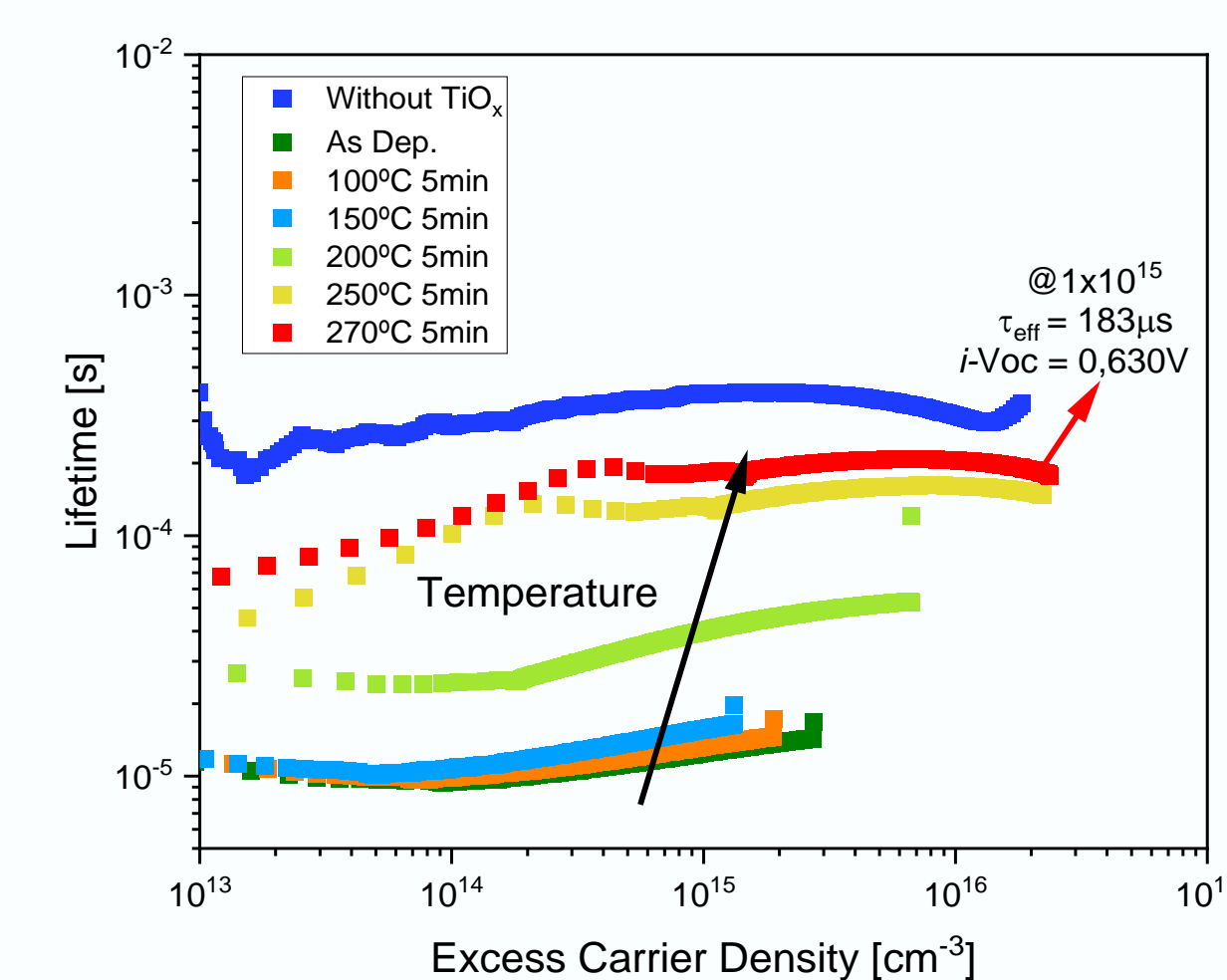
With the samples of 6min HPS,  $\rho_c \sim 10 \text{ m}\Omega\text{cm}^2$ , that is within the range of what has been reported with ALD  $\text{TiO}_x$  [3]



### QSS-Photoconducance

To measure the carrier lifetime of  $\text{TiO}_x$  + amorphous Si. Quality of interface i.e., quantity of dangling bonds (unpassivated bonds)

As deposited  $\text{TiO}_x$  reduce lifetime, but temperature annealing might recover.



## Conclusions

- We successfully fabricated high pressure sputtered  $\text{TiO}_x$  with a 2-step process. The temperature and the time of oxidation play an important role to achieve a  $\text{TiO}_x$  almost stoichiometric as XPS shows.
- FTIR and TEM image depict that the  $\text{TiO}_x$  film is principally amorphous with embedded nanocrystals. When a higher temperature is applied (i.e., 200°C) the film tends to grow showing some nanocrystalline arrangements.
- We fabricated Cox&Strack structure to measure the specific contact resistivity ( $\rho_c$ ) between n-Si and our  $\text{TiO}_x$ . The samples of 5nm show the lower  $\rho_c \sim 10 \text{ m}\Omega\text{cm}^2$ , this is in accordance with values obtained with  $\text{TiO}_x$  fabricated with ALD. Thinner films lead to higher  $\rho_c$  values, most likely due to enhanced substrate oxidation.
- We measured the carrier lifetime of  $\text{TiO}_x$  + a-Si:H(i). A priori the deposition of  $\text{TiO}_x$  reduce the lifetime, but annealing shows a recovery. The use of a-Si:H (i) appears as a good approach to obtain high lifetime for the use of  $\text{TiO}_x$  in selective contacts solar cells structure.

## References

- [1] Matsui, T., Bivour, M., Ndione, P. F., Bonilla, R. S., & Hermle, M. (2020). Origin of the tunable carrier selectivity of atomic-layer-deposited  $\text{TiO}_x$  nanolayers in crystalline silicon solar cells. *Solar Energy Materials and Solar Cells*, 209(November 2019), 110461. <https://doi.org/10.1016/j.solmat.2020.110461>
- [2] Zhang, J. Y., et al. (2002). Nanocrystalline  $\text{TiO}_2$  films studied by optical, XRD and FTIR spectroscopy. *Journal of Non-Crystalline Solids*, 303(1), 134–138.
- [3] Titova, V., et al. (2017). Effective passivation of crystalline silicon surfaces by ultrathin atomic-layer-deposited  $\text{TiO}_x$  layers. *Energy Procedia*, 124, 441–447.

The authors acknowledge the "CAI de Técnicas Físicas" of Universidad Complutense de Madrid for ion implantation, RTA annealing and e-beam evaporation. Also, the "Centro de Espectroscopia y Correlación" for the FTIR measures, the CENIM -CSIC for the XPS measures and analysis and CNME for the TEM images. This project was funded by AEI through the projects PID2020-116508RB-I00, PID2020-117498RB-I00 and TED2021-130894B-C21. F. Pérez-Zenteno acknowledges the predoctoral contract from UCM (call CT58/21-CT59/21) and CONACYT Mexican grants program. D. Caudevilla would also acknowledge the Grant PRE2018-0.83798, financed by MICINN and European Social Fund.